JOURNAL OF MATERIALS SCIENCE 30 (1995) 4793–4800

Matrix cracking with frictional bridging fibres in continuous fibre ceramic composites

Part II Cracking due to residual stresses

C. H. HSUEH
Metals and Ceramics Division, Oak Ridge National Laboratory, Oak Ridge, TN 37831, USA

Interfacial debonding and matrix cracking due to residual axial stresses have been analysed for unidirectional fibre-reinforced ceramic composites. The analytical solutions for the crack-opening displacement, the axial displacement of the composite due to interfacial debonding, and the critical residual axial stress for matrix cracking have been obtained. The solutions were then compared with those for tensile loading in the fibre direction. Three issues related to Part I, i.e. the effective fracture toughness of the composite, the critical loading stress for matrix cracking in the presence of residual stresses, and the debonded fibre length due to loading, were also addressed in the present study.

1. Introduction

Matrix cracking bridged by intact fibres, which debond from the matrix and then slip frictionally against the matrix, was analyzed in Part I [1] for unidirectional fibre-reinforced ceramic composites under tensile loading parallel to the fibre axis. The effect of bonding at the fibre–matrix interface, Poissons's effect of the fibre, and residual stresses were included in the analysis [1]. The premise of the analyses in Part I was that interfacial debonding and matrix cracking do not occur prior to loading. The case of matrix cracking due to residual axial stresses has been analysed elsewhere; however, the interfacial bonding was ignored in the analysis [2].

As a complement to Part I, the purpose of the present study was to analyse the critical residual axial stress for steady state (i.e. long) matrix cracking. Interfacial bonding has been included in the analysis. The existing solution [2] can be recovered by ignoring interfacial bonding in the present solution. Also, three issues related to Part I were addressed in this study. First, the effective fracture toughness of the composite has been derived which is essential in solving the matrix cracking problem for short cracks [3–7]. Second, while the effects of the residual axial stress on the critical loading stress for matrix cracking was addressed qualitatively in Part I, its analytical expression was determined in this study. Third, the debonded fibre length at the critical loading stress for matrix cracking has been analysed. This debonded fibre length defines the minimum fibre length required in order to ensure full development of the fibre bridging stress during matrix cracking.

2. Analyses

A schematic representation of steady state matrix cracking due to residual stresses is shown in Fig. 1 for unidirectional composites. The matrix crack is bridged by intact fibres, and the shaded areas at the interface represent interfacial debonding (Fig. 1). To achieve matrix cracking, the residual axial stress in the matrix must be tensile. Accordingly, the residual axial stress in the fibre is compressive in order to satisfy the equilibrium condition. These residual stresses can occur when the thermal expansion coefficient of the matrix is greater than that of the fibre and the composite is cooled from its fabrication temperature. The residual axial stresses are zero at the crack surface, increase with the axial distance from the crack surface, and reach equilibrium values, σ_{fz} and σ_{mz}, respectively, in the fibre and the matrix, at a distance sufficiently remote from the crack surface (Fig. 1). The crack-opening displacement, $2u_0$, and the additional displacement, u_{debond}, in the loading direction on each side of the composite due to debonding and sliding at the fibre–matrix interface are also shown.

The representative volume element used in Part I is used to model the problem depicted in Fig. 1. A fibre with a radius, a, is located at the centre of a coaxial cylindrical shell of matrix with an outer radius, b, such that a^2/b^2 corresponds to the volume fraction of fibres, V_f (Fig. 2a). During cooling, the composite has a displacement, u_{bonded}, in the axial direction when the interface remains bonded (Fig. 2b). In the presence of interfacial debonding, partial relaxation of the thermal stress occurs which, in turn, results in an axial displacement of the composite, u_{debond}. Both the half crack-opening displacement, u_0, and the axial

0022–2461

displacement of the composite due to interfacial debonding, u_{debond}, are shown in Fig. 2c.

2.1. Residual axial stresses

The residual axial stresses in the fibre and the matrix, σ_f and σ_m, are both functions of the axial position, z. The mechanical equilibrium condition requires that

$$V_f\sigma_f + V_m\sigma_m = 0 \tag{1}$$

where V_m $(= 1 - V_f)$ is the volume fraction of the matrix. Depending upon the boundary condition (i.e. bonded or debonded) at the interface, the residual axial stresses can be determined accordingly.

2.1.1. The bonded interface

The residual axial stresses in the fibre and the matrix have their equilibrium values, σ_{fz} and σ_{mz}. Continuity of the axial strain is required for the bonded interface, such that

$$\frac{\sigma_{fz}}{E_f} + \alpha_f\Delta T = \frac{\sigma_{mz}}{E_m} + \alpha_m\Delta T \tag{2}$$

where E and α are Young's modulus and the thermal expansion coefficient, the subscripts, f and m, denote the fibre and the matrix, respectively, and ΔT is the cooling temperature range over which stresses can be developed. Combination of Equations 1 and 2 yields

$$\sigma_{fz} = \frac{-V_m E_f E_m \varepsilon_T}{E_C} \tag{3a}$$

$$\sigma_{mz} = \frac{V_f E_f E_m \varepsilon_T}{E_C} \tag{3b}$$

where

$$E_C = V_f E_f + V_m E_m \tag{4}$$

and $\varepsilon_T = (\alpha_f - \alpha_m)\,\Delta T$ is the thermal mismatch strain (and is also the transformation strain defined in Part I) between the fibre and the matrix.

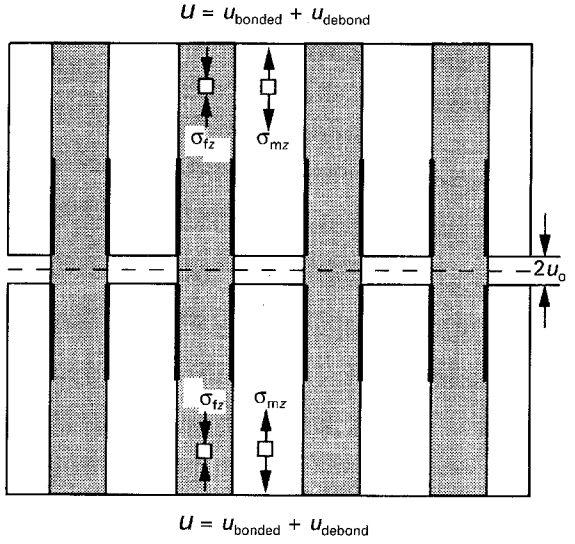

Figure 1 Schematic illustration of residual stress-induced interfacial debonding and a steady-state matrix crack bridged by intact fibres.

2.1.2. The debonded interface

Interfacial debonding occurs when the axial mismatch strain between the fibre and the matrix reaches a critical value, ε_d [8], which can be related to the energy release rate for interfacial debonding, G_i, by [9, 10]

$$\varepsilon_d = 2\left(\frac{E_C G_i}{aV_m E_f E_m}\right)^{1/2} \tag{5}$$

Interfacial debonding with a debonded zone length, h, is shown in Fig. 2c. The residual axial stresses in the fibre and the matrix are both zero at the crack surface (i.e. at $z = h$). At the end of the debonding zone (i.e. at $z = 0$), the residual axial stresses in the fibre and the

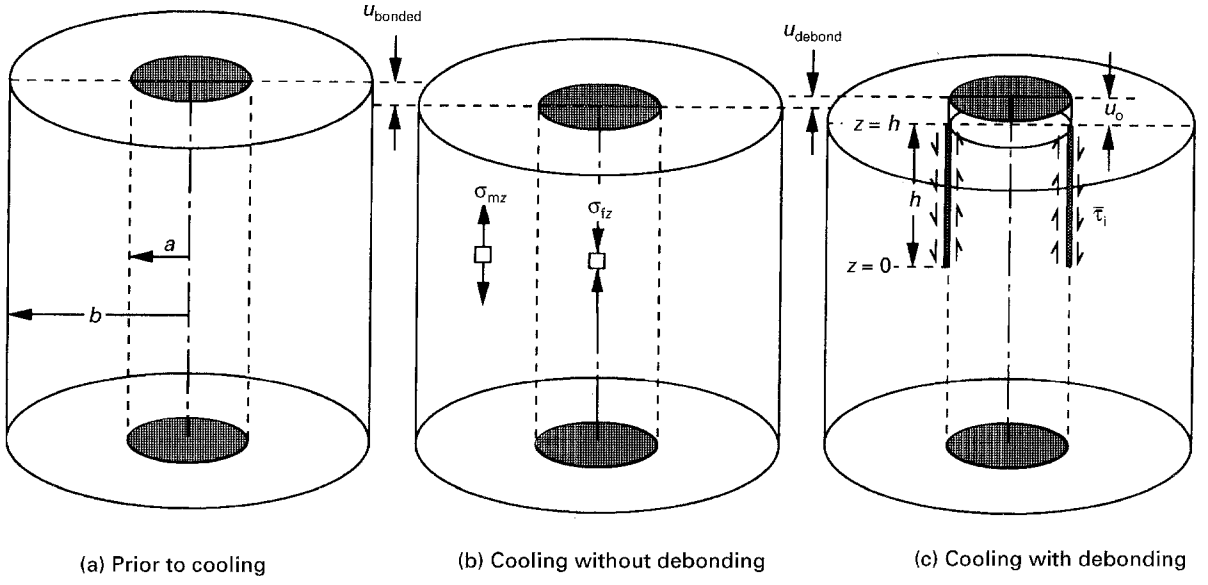

Figure 2 A representative volume element for the problem of residual stress-induced interfacial debonding and matrix cracking, (a) prior to cooling, (b) cooling without interfacial debonding, and (c) cooling with interfacial debonding. The half crack opening displacement, u_0, and the displacement of the composite due to interfacial debonding, u_{debond}, are also shown.

matrix, σ_{fd} and σ_{md}, satisfy the following relation

$$\frac{\sigma_{fd}}{E_f} + \alpha_f \Delta T - \frac{\sigma_{md}}{E_m} - \alpha_m \Delta T = \varepsilon_d \quad (6)$$

Combination of Equations 1, 2, 5 and 6 yields

$$G_i = \frac{aE_C(\sigma_{fd} - \sigma_{fz})^2}{4V_m E_f E_m} \quad (7)$$

In the absence of interfacial bonding (i.e. $G_i = 0$), the residual axial stress in the fibre at the end of the sliding zone has the equilibrium value (i.e. $\sigma_{fd} = \sigma_{fz}$, see Equation 7).

For a frictional interface, an average Poisson's effect was adopted in Part I such that the interfacial frictional stress is dictated by an average value, $\bar{\tau}_i$. The residual axial stresses in the fibre and the matrix, σ_f and σ_m, are

$$\sigma_f = \left(1 - \frac{z}{h}\right)\sigma_{fd} \qquad \text{for } 0 \leqslant z \leqslant h \quad (8a)$$

$$\sigma_m = \left(1 - \frac{z}{h}\right)\sigma_{md} \qquad \text{for } 0 \leqslant z \leqslant h \quad (8b)$$

where the sliding zone length, h, can be determined by the stress transfer equation, such that

$$h = \frac{a\sigma_{fd}}{2\bar{\tau}_i} \quad (9)$$

It is noted that σ_{fd} is compressive (i.e. negative), and $\bar{\tau}_i$ is negative due to the coordinate system (Fig. 2c) used in the present study. In the bonded zone (i.e. $z \leqslant 0$), σ_f and σ_m increase quickly from σ_{fd} and σ_{md} to their equilibrium values, σ_{fz} and σ_{mz}, respectively [11–13].

2.2. The displacements

Both the crack-opening displacement and the displacement of the composite due to interfacial debonding are derived as follows.

2.2.1. The crack-opening displacement

The crack opening displacement is dictated by the relative axial displacement between the fibre and the matrix at the crack surface. The axial displacements of the fibre and the matrix at the crack surface, $w_f(h)$ and $w_m(h)$, due to sliding can be obtained by integration of the axial strains along the sliding length, such that

$$w_f(h) = h\left(\frac{\sigma_{fd}}{2E_f} + \alpha_f \Delta T\right) \quad (10a)$$

$$w_m(h) = h\left(\frac{\sigma_{md}}{2E_m} + \alpha_m \Delta T\right) \quad (10b)$$

It can be derived that the half crack opening displacement (Fig. 2c), u_0 ($= w_f(h) - w_m(h)$), is

$$u_o = \frac{aE_C\sigma_{fd}}{2V_m E_f E_m \bar{\tau}_i}\left(\frac{\sigma_{fd}}{2} - \sigma_{fz}\right) \quad (11)$$

In the absence of interfacial bonding (i.e. $\sigma_{fd} = \sigma_{fz}$), Equation 11 becomes

$$u_o = \frac{-aE_C\sigma_{fz}^2}{4V_m E_f E_m \bar{\tau}_i} \quad (12)$$

2.2.2. The displacement of the composite due to debonding

This is the relative axial displacement between the composites with and without debonding. When the interface remains bonded, the axial strain in the composite, ε_C, is described by Equation 2, and the corresponding axial displacement, w_C, within a length h is

$$w_C(h) = h\left(\frac{\sigma_{fz}}{E_f} + \alpha_f \Delta T\right) \quad (13)$$

It can be derived that the additional axial displacement of the composite due to debonding (Fig. 2c), u_{debond}($= w_f(h) - w_C(h)$), becomes

$$u_{debond} = \frac{a\sigma_{fd}}{2E_f\bar{\tau}_i}\left(\frac{\sigma_{fd}}{2} - \sigma_{fz}\right) \quad (14)$$

In the absence of interfacial bonding (i.e. $\sigma_{fd} = \sigma_{fz}$), Equation 14 becomes

$$u_{debond} = \frac{-a\sigma_{fz}^2}{4E_f\bar{\tau}_i} \quad (15)$$

2.3. The matrix cracking stress

The energy-based criterion [2–7] has been adopted to analyse the critical stress required for steady-state matrix cracking. For the problem considered in the present study, the following energy terms are involved: (1) $U_{f(r)}$ and $U_{m(r)}$, the elastic strain energies in the fibre and the matrix due to residual stresses, (2) U_s, the energy due to sliding at the debonded interface, (3) G_m, the energy release rate for matrix cracking, and (4) G_i, the energy release rate for interfacial debonding.

To adopt the energy-based cracking criterion, a steady-state matrix crack in a long specimen of unit depth is considered (Fig. 3) [14]. The crack extends through the depth of the specimen with a straight front. Under residual stresses, the crack advances a distance dc. For steady-state cracking, the stress at the crack front remains unchanged during crack extension, and the stresses far behind and ahead of the crack front also remain unchanged. Hence, the energy changes in the specimen due to crack extension are the differences in energy between two strips, which are, respectively, far behind and ahead of the crack front, of thicknesses dc. In the strip far ahead of the crack front, the fibre and the matrix remain bonded. In the strip far behind the crack front, interfacial debonding and sliding occur within a length of $2h$ which is denoted by a shaded region in Fig. 3. Hence, to analyse the energy difference between these two strips, it is sufficient to consider the two shaded regions in Fig. 3 which are designated as Regions I and II, respectively, for the regions ahead of and behind of the crack front.

During crack extension and interfacial debonding, the stress changes in the fibre and the matrix are

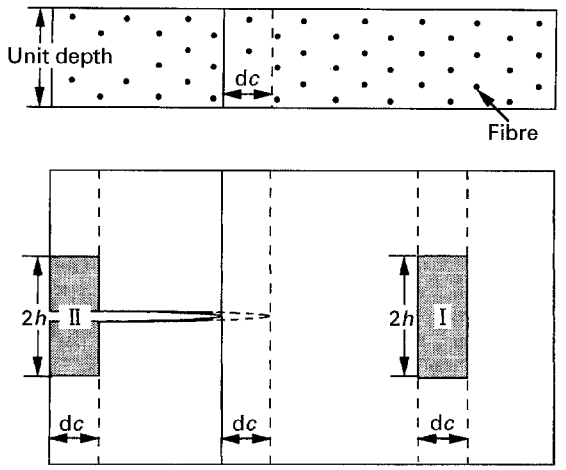

Figure 3 Schematic illustration of a steady-state matrix crack, which is induced by residual stresses, in a long specimen of unit depth to analyse the matrix cracking stress.

significant only in the axial direction. Hence, the energy due to only the axial stress is considered for the fibre and the matrix.

2.3.1. The elastic strain energy

In region I, the fibre and the matrix remain bonded, and the residual axial stresses in the fibre and the matrix, σ_{fz} and σ_{mz}, are uniform along the axial direction. The elastic strain energy density in the fibre and the matrix are $\sigma_{fz}^2/2E_f$ and $\sigma_{mz}^2/2E_m$, respectively. With unit depth, the volume in region I is $2hdc$. Because the fibre and the matrix have the volume fractions of V_f and V_m, respectively, the corresponding elastic strain energies, $U_{f(r1)}$ and $U_{m(r1)}$, in region I are

$$U_{f(r1)} = \frac{hV_f\sigma_{fz}^2 dc}{E_f} \tag{16a}$$

$$U_{m(r1)} = \frac{hV_m\sigma_{mz}^2 dc}{E_m} \tag{16b}$$

The total elastic strain energy in region I becomes

$$U_{f(r1)} + U_{m(r1)} = \frac{hV_f E_C \sigma_{fz}^2 dc}{V_m E_f E_m} \tag{17}$$

Equation 17 is identical to Equation A4 in Part I, which was derived by using the Eshelby model [15].

In region II, interfacial debonding and sliding occur. The axial stresses in the fibre and the matrix, σ_f and σ_m, are described by Equations 8a and b, respectively. The total elastic strain energy in the fibre and the matrix, $U_{f(r2)} + U_{m(r2)}$, is

$$U_{f(r2)} + U_{m(r2)} = \frac{V_f dc}{E_f}\int_0^h \sigma_f^2 dz + \frac{V_m dc}{E_m}\int_0^h \sigma_m^2 dz \tag{18}$$

Substitution of Equations 8a and b into Equation 18 yields

$$U_{f(r2)} + U_{m(r2)} = \frac{hV_f E_C \sigma_{fd}^2 dc}{3V_m E_f E_m} \tag{19}$$

The elastic strain energy difference between regions II and I, $dU_{f(r)} + dU_{m(r)}$, is hence

$$dU_{f(r)} + dU_{m(r)} = \frac{hV_f E_C(\sigma_{fd}^2 - 3\sigma_{fz}^2)dc}{3V_m E_f E_m} \tag{20}$$

2.3.2. The sliding energy

The sliding energy exists in region II but not in region I. In region II, the axial displacements result from both the axial stresses described by Equation 8 and the stress-free thermal strains, and the solutions are

$$w_f(z) = z\left[\frac{(2h - z)\sigma_{fd}}{2hE_f} + \alpha_f \Delta T\right] \quad 0 \leqslant z \leqslant h \tag{21a}$$

$$w_m(z) = z\left[\frac{(2h - z)\sigma_{md}}{2hE_m} + \alpha_m \Delta T\right] \quad 0 \leqslant z \leqslant h \tag{21b}$$

Energy is dissipated due to the relative displacement between the fibre and the matrix under an average interfacial frictional stress, $\bar{\tau}_i$. The sliding energy in region II is equal to the change in the sliding energy due to crack extension, such that

$$dU_S = \frac{-4adc}{b^2}\int_0^h \bar{\tau}_i(w_f - w_m)dz \tag{22a}$$

where the negative sign is due to the negative value of $\bar{\tau}_i$. Substitution of Equations 1, 9 and 21 into Equation 22a yields

$$dU_S = \frac{hV_f E_C \sigma_{fd}(3\sigma_{fz} - 2\sigma_{fd})dc}{3V_m E_f E_m} \tag{22b}$$

2.3.3. The energy release rates for matrix cracking and interfacial debonding

In region II, the energy required for matrix cracking and interfacial debonding, dG_m and dG_i, are

$$dG_m = V_m G_m dc \tag{23a}$$

$$dG_i = \frac{4ahG_i dc}{b^2} \tag{23b}$$

Substitution of Equation 7 into Equation 23b yields

$$dG_i = \frac{hV_f E_C(\sigma_{fd} - \sigma_{fz})^2 dc}{V_m E_f E_m} \tag{24}$$

2.3.4. The matrix cracking stress

The critical residual axial stress in the fibre, $\sigma_{fz(c)}$, required for matrix cracking, can be obtained from the energy balance relation, such that

$$dU_{f(r)} + dU_{m(r)} + dU_S + dG_m + dG_i = 0$$

$$\text{at } \sigma_{fz} = \sigma_{fz(c)} \tag{25}$$

Substitution of Equations 20, 22b, 23a and 24 into Equation 25 yields

$$[3\sigma_{fz(c)} - 2\sigma_{fd}]\sigma_{fd}^2 = \frac{6\bar{\tau}_i V_m^2 E_f E_m G_m}{aV_f E_C} \tag{26}$$

In the absence of interfacial bonding, Equation 26 becomes

$$\sigma_{fz(c)} = \left(\frac{6\bar{\tau}_i V_m^2 E_f E_m G_m}{a V_f E_C}\right)^{1/3} \quad (27a)$$

The corresponding critical residual axial stress in the matrix, $\sigma_{mz(c)}$, for matrix cracking is

$$\sigma_{mz(c)} = \left(\frac{-6\bar{\tau}_i V_f^2 E_f E_m G_m}{a V_m E_C}\right)^{1/3} \quad (27b)$$

Equation 27b is identical to the result derived by Aveston *et al.* [2].

3. Comparison

The displacements and matrix cracking due to residual axial stresses are now compared to those due to axial loading derived in Part I.

3.1. Matrix cracking due to axial loading

When the axial loading stress on the fibre is σ_0, the half crack-opening displacement, u_0, and the displacement of the composite due to interfacial debonding, u_{debond}, have been derived, such that [1]

$$u_0 = \frac{-aV_m E_m(\sigma_0^2 - \sigma_d^2)}{4E_f E_C \bar{\tau}_i} \quad (28a)$$

$$u_{debond} = \frac{-aV_m^2 E_m^2(\sigma_0^2 - \sigma_d^2)}{4E_f E_C^2 \bar{\tau}_i} \quad (28b)$$

where σ_d is the loading stress on the fibre to initiate interfacial debonding. The critical axial loading stress on the fibre, σ_{cri}, for matrix cracking is dictated by [1]

$$\sigma_{cri}^3 - 3\sigma_d^2\sigma_{cri} + 2\sigma_d^3 = \frac{-6\bar{\tau}_i E_f E_C^2 G_m}{a V_f V_m E_m^2} \quad (28c)$$

The functional dependences of Equation 28a–c are different from those of Equations 11, 14 and 26. However, it is noted that whereas the axial load at the crack surface is carried by the fibre only, the residual axial stresses exist in both the fibre and the matrix. To avoid this difference in the "stress mode", the "strain mode" is considered as follows.

Using the "strain mode" and Equation 5 (which relates ε_d and hence σ_d to G_i), Equation 28a–c can be rewritten as

$$u_0 = \frac{-aV_m E_f E_m \varepsilon_0^2}{4E_C \bar{\tau}_i} + \frac{G_i}{\bar{\tau}_i} \quad (29a)$$

$$u_{debond} = \frac{-aV_m^2 E_f E_m^2 \varepsilon_0^2}{4E_C^2 \bar{\tau}_i} + \frac{V_m E_m G_i}{E_C \bar{\tau}_i} \quad (29b)$$

$$\varepsilon_{cri}^3 - \frac{12E_C G_i \varepsilon_{cri}}{aV_m E_f E_m} + 16\left(\frac{E_C G_i}{aV_m E_f E_m}\right)^{3/2} = \frac{-6\bar{\tau}_i E_C^2 G_m}{aV_f V_m E_f^2 E_m^2} \quad (29c)$$

where $\varepsilon_0 = \sigma_0/E_f$ and $\varepsilon_{cri} = \sigma_{cri}/E_f$. Equations 29a–c will be used for comparison with those due to residual axial stresses obtained in Section 3.2.

3.2. Matrix cracking due to residual axial stresses

Using Equations 3a and 7, Equations 11, 14 and 26 can be rewritten as

$$u_0 = \frac{-aV_m E_f E_m \varepsilon_T^2}{4E_C \bar{\tau}_i} + \frac{G_i}{\bar{\tau}_i} \quad (30a)$$

$$u_{debond} = \frac{-aV_m^2 E_f E_m^2 \varepsilon_T^2}{4E_C^2 \bar{\tau}_i} + \frac{V_m E_m G_i}{E_C \bar{\tau}_i} \quad (30b)$$

$$\varepsilon_{T(C)}^3 - \frac{12E_C G_i \varepsilon_{T(C)}}{aV_m E_f E_m} + 16\left(\frac{E_C G_i}{aV_m E_f E_m}\right)^{3/2} = \frac{-6\bar{\tau}_i E_C^2 G_m}{aV_f V_m E_f^2 E_m^2} \quad (30c)$$

where $\varepsilon_{T(C)}$ is related to $\sigma_{fz(c)}$ by Equation 3a. It is noted that Equation 29a–c are identical to Equation 30a–c when ε_0 and ε_{cri} are replaced by ε_T and $\varepsilon_{T(C)}$, respectively.

4. Extension of Part I

Three issues related to Part I, i.e. the effective fracture toughness of the composite, the critical loading stress for matrix cracking in the presence of residual stresses, and the debonded fibre length at matrix cracking due to loading, are addressed in this section.

4.1. The effective fracture toughness of the composite

The matrix cracking stress derived in the present study is steady state, i.e. a long crack asymptote. To derive the matrix cracking stress for a short crack, three steps are involved [3–7]. First, a relation between the fibre bridging stress and the crack opening displacement is required. Second, based on the bridging stress–crack opening displacement relation, an iterative numerical calculation is required to derive a self-consistent crack profile and bridging stress at a given applied stress. Third, the stress intensity is calculated from the self-consistent bridging stress which is then equated to the effective composite toughness to derive the matrix cracking stress. Based on the above procedures, the matrix cracking stress for a short crack has been analysed elsewhere [3–7]. However, different results have been obtained. These differences are due to the adoption of different effective composite toughnesses. This effective composite toughness is addressed as follows.

Two different relations between the fracture toughness of the composite and of the matrix, K_C and K_m, have been derived [3, 4]. By assuming that the strains in the composite and the matrix are the same in the region immediately ahead of the crack, and that the toughness scales with the stress, the $K_C - K_m$ relation is [3]

$$K_C = \frac{E_C K_m}{E_m} \quad (31)$$

By considering the energy required to grow the matrix crack, the result derived by McCartney is [4]

$$K_C = \left(\frac{V_m E_C}{E_m}\right)^{1/2} K_m \quad (32)$$

It has been discussed that McCartney's result is energetically consistent [4].

Including interfacial bonding in the present analysis, interfacial debonding is required during matrix cracking. The energy required to crack the matrix and to debond the interface is

$$G_C = V_m G_m + \frac{4ahG_i}{b^2} \quad (33)$$

where the debonded length, h, and the energy release rate for interfacial debonding, G_i, have been defined, respectively, by Equations 17b and 34 in Part I. The energy release rates for cracking, G_m and G_C, can be related to toughnesses, K_m and K_C, by

$$K_m = (E_m G_m)^{1/2} \quad (34a)$$

$$K_C = (E_C G_C)^{1/2} \quad (34b)$$

Substitution of h, G_i, and Equation 34a and b into Equation 33 yields

$$K_C = \left[\frac{V_m E_C}{E_m} - \frac{2V_f V_m(\sigma_0 - \sigma_d)G_i}{\bar{\tau}_i G_m}\right]^{1/2} K_m \quad (35)$$

In the absence of interfacial bonding, $G_i = 0$ and McCartney's result (i.e. Equation 32) is recovered.

4.2. The critical loading stress for matrix cracking in the presence of residual stresses

Ignoring the interfacial bonding, the effect of the residual axial stresses on the critical loading stress for matrix cracking has been addressed; however, the analytical solution was not explicitly given [1]. This solution is given as follows.

The matrix cracking stress due to both applied stress and residual axial stresses can be obtained by substituting Equations 28, 30b, 33a, 35 and A10 into Equation A11 in Part I, such that

$$\left(\sigma_{cri} - \frac{E_C \sigma_{fz}}{V_m E_m}\right)^3 + \left(\frac{E_C \sigma_{fz}}{V_m E_m}\right)^3 = \frac{-6\bar{\tau}_i E_f E_C^2 G_m}{aV_f V_m E_m^2} \quad (36)$$

When the residual axial stress is small compared with the loading stress, the second term on the left-hand side of Equation 36 can be ignored, such that

$$\sigma_{cri} - \frac{E_C \sigma_{fz}}{V_m E_m} = \left(\frac{-6\bar{\tau}_i E_f E_C^2 G_m}{aV_f V_m E_m^2}\right)^{1/3} \quad (37)$$

Furthermore, using the relation between σ_{fz} and σ_{mz} described by Equation 1, Equation 37 can be converted to

$$\sigma_{cri}^{\infty} + \frac{E_C \sigma_{mz}}{E_m} = \left(\frac{-12\bar{\tau}_i V_f^2 E_f E_C^2 \gamma_m}{aV_m E_m^2}\right)^{1/3} \quad (38)$$

where σ_{cri}^{∞} ($= V_f \sigma_{cri}$) is the critical applied stress on the composite for matrix cracking, and γ_m($= G_m/2$) is the fracture surface energy of the matrix. Equation 38 is identical to the result derived by Budiansky *et al.* [14].

4.3. The debonded fibre length at matrix cracking due to loading

Interfacial debonding and friction occur during matrix cracking. The premise of the matrix cracking stress derived in Part I is that the fibre is sufficiently long for interfacial debonding and sliding to occur. To ensure this premise, it is crucial to have a knowledge of the debonded fibre length when steady-state matrix cracking occurs. The relation between the debonded length to fibre radius ratio and the energy release rate ratio of interfacial debonding to matrix cracking (i.e. h/a and G_i/G_m) has been addressed elsewhere; however, interfacial friction was ignored [14]. Including interfacial friction, the debonded fibre length at matrix cracking due to loading is addressed as follows.

To reduce the number of parameters, the residual stress is ignored. However, an approximate residual stress effect can be included by replacing σ_{cri}^{∞} with $\sigma_{cri}^{\infty} + E_C \sigma_{mz}/E_m$ (see Equation 38) in the solution. The h/a versus G_i/G_m relation can be obtained by satisfying the following three Equations. First, the equation dictating the critical loading stress on the fibre, σ_{cri}, for matrix cracking is [1]

$$\sigma_{cri}^3 - 3\sigma_d^2 \sigma_{cri} + 2\sigma_d^3 = \sigma_{cri(0)}^3 \quad (39)$$

where $\sigma_{cri(0)}$ is the critical loading stress on the fibre for matrix cracking when the interface is unbounded, and is given by [1]

$$\sigma_{cri(0)} = \left(\frac{-6\bar{\tau}_i E_f E_C^2 G_m}{aV_f V_m E_m^2}\right)^{1/3} \quad (40)$$

Second, the loading stress on the fibre, σ_d, to initiate interfacial debonding can be related to G_i by [1]

$$\sigma_d = 2\left(\frac{E_f E_C G_i}{aV_m E_m}\right)^{1/2} \quad (41)$$

Third, the debonded fibre length, h, is [1]

$$h = \frac{-aV_m E_m(\sigma_{cri} - \sigma_d)}{2E_C \bar{\tau}_i} \quad (42)$$

The h/a versus G_i/G_m relation can be obtained from Equations 39, 41 and 42, and the results are shown as follows.

The critical applied stress on the composite, σ_{cri}^{∞}, for matrix cracking has been measured for Nicalon fibre-reinforced lithium aluminosilicate (LAS) composite [16, 17]. The material properties pertinent to this composite are: $E_f = 200$ GPa, $E_m = 85$ GPa, $V_f = 0.5$, $a = 8$ μm, $G_m = 44$ N m^{-1}, and $-\bar{\tau}_i = 2$ MPa [16]. Also, this composite has negligible residual stresses [16]. Unless noted otherwise, these materials properties will be adopted below to examine the essential trends of the debonded fibre length, h.

4.3.1. The Nicalon/LAS composites

The debonded fibre length, h, as a function of G_i is calculated and shown in Fig. 4 for Nicalon/LAS composites. The critical applied stresses on the composite for matrix cracking, σ_{cri}^{∞}, and for interfacial debonding, σ_d^{∞} ($= V_f \sigma_d$) , are also shown. Both σ_{cri}^{∞} and σ_d^{∞} increase and h decreases with the increase in G_i. When

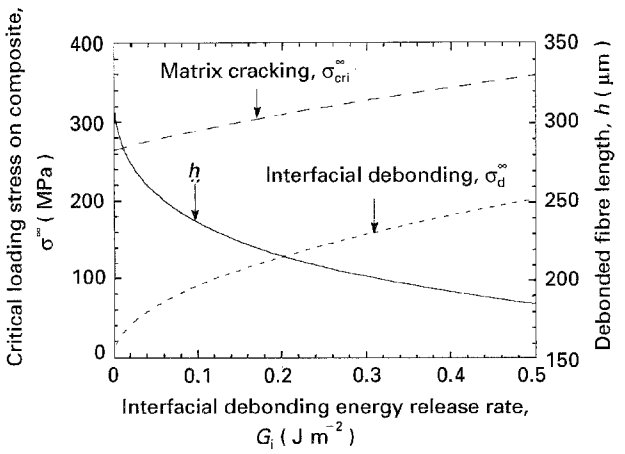

Figure 4 The debonded fibre length, h, the critical applied stresses on the composite for matrix cracking, σ_{cri}^{∞}, and for interfacial debonding, σ_d^{∞}, as functions of the energy release rate for interfacial debonding, G_i, for Nicalon/LAS composites.

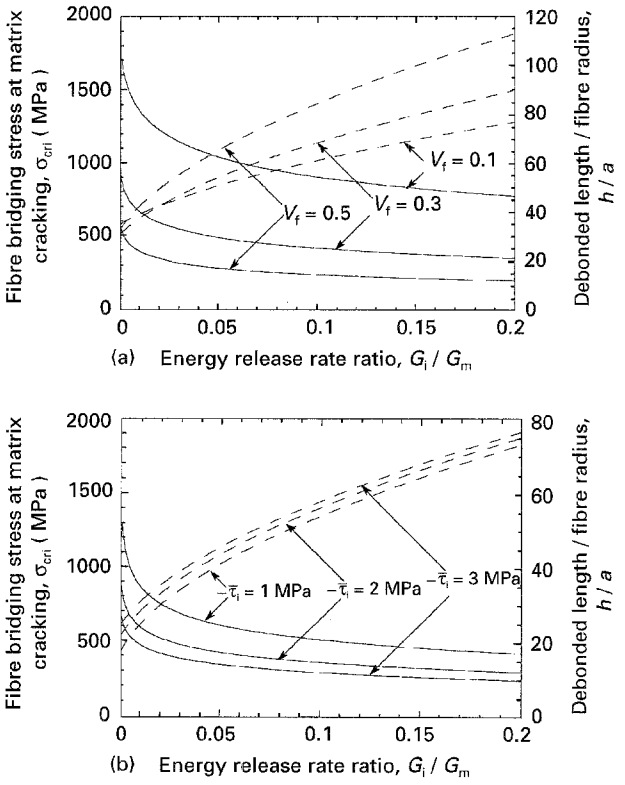

Figure 5 (—) The normalized debonded fibre length, h/a, and (- - -) the critical loading stress in the fibre for matrix cracking, σ_{cri}, as functions of the energy release rate ratio, G_i/G_m, at different values of (a) fibre volume fraction, V_f, and (b) interfacial frictional stress $-\bar{\tau}_i$.

the interface is unbonded, the critical applied stress on the composite for matrix cracking, $\sigma_{cri(0)}^{\infty}$ ($= V_f\sigma_{cri(0)}$), can be calculated from Equation 40 and is 265 MPa. The measured σ_{cri}^{∞} is ~290 MPa [16]. Because the residual stress is negligible [16], the difference between $\sigma_{cri(0)}^{\infty}$ and σ_{cri}^{∞} could be due to interfacial bonding. Based on the measured σ_{cri}^{∞} and Fig. 4, G_i is ~0.1 J m^{-2} and h = ~240 μm. These results are in agreement with the experimental evaluations [16] of G_i being less than 0.4 J m^{-2} and h being greater than 200 μm. It is noted that the loading stress on the composite for debonding, σ_d^{∞}, is significant (~90 MPa) even when G_i is small (~0.1 J m^{-2}). This is due to the small radius of the fibre (see Equation 41).

4.3.2. *Effects of* V_f and $\bar{\tau}_i$ on h/a

When the volume fraction of fibres is changed, or the interface has been modified [18–20] such that the interfacial frictional stress is changed, the debonded fibre length will be changed accordingly. The ratio of debonded fibre length to fibre radius, h/a, as a function of the energy release rate ratio, G_i/G_m, is shown in Fig. 5a and b, respectively, at different values of V_f and $\bar{\tau}_i$. When the volume fraction of fibres or the interfacial frictional stress is decreased, longer fibres are required to ensure full development of the bridging stress in the fibre during matrix cracking. The critical loading stress on the fibre, σ_{cri}, for matrix cracking is also shown in Fig. 5. It is noted that σ_{cri} should not exceed the tensile strength of the fibre (~2 GPa for Nicalon fibres [21]). Otherwise, fibre fracture occurs before matrix cracking.

5. Conclusion

When the matrix has a greater thermal expansion coefficient than the fibre, residual axial tension and compression are induced, respectively, in the matrix and the fibre during cooling. Interfacial debonding and matrix cracking due to these residual axial stresses are analysed for unidirectional fibre-reinforced ceramic composites in the present study. Three analytical solutions are derived: (a) the crack-opening displacement, u_0, (b) the axial displacement of the composite due to interfacial debonding, u_{debond}, and (c) the critical residual axial stress in the fibre for matrix cracking, $\sigma_{fz(c)}$. The corresponding solutions due to axial loading have been derived in Part I, i.e. (a) u_0, (b) u_{debond}, and (c) the critical axial loading stress on the fibre for matrix cracking, σ_{cri}. It is noted that solutions of residual stress-induced cracking (see Equation 30a–c) become identical to those of load-induced cracking (see Equation 29a–c) when the loading strain in the fibre, ε_0, in the latter case is replaced by the mismatch strain between the fibre and the matrix, ε_T, in the former case. The existing solution for matrix cracking due to residual axial stresses [2] can be recovered by ignoring the interfacial bonding in the present solution.

Three issues related to Part I have been addressed. First, the effective toughness of the composite, K_C, has been derived which is essential in analysing the matrix cracking stress for short cracks. Considering the energy required to crack the matrix and to debond the interface, the present solution of K_C agrees with McCartney's solution [4] when interfacial bonding is ignored in the present solution. Second, ignoring the interfacial bonding, the analytical solution of the critical loading stress for matrix cracking in the presence of residual stresses has been given. When the residual stress is small compared to the critical loading stress, the existing solution [14] is recovered. Third, the debonded fibre length at matrix cracking due to loading has been analysed. This solution is required to

ensure that the fibre is sufficiently long for interfacial debonding and sliding to occur during matrix cracking.

Acknowledgements

The author thanks Drs P. F. Becher, K. P. Plucknett and E. Lara-Curzio, for reviewing the manuscript. The research was jointly sponsored by the US Department of Energy, Division of Materials Sciences, Office of Basic Energy Sciences, and Assistant Secretary for Energy, Efficiency and Renewable Energy, Office of Industrial Technologies, Energy Efficiency Division and Continuous Fiber Ceramic Composites Program, under contract DE-AC05-84OR21400 with Martin Marietta Energy Systems, Inc.

References

1. C. H. HSUEH, *J. Mater. Sci.*, **30** (1995) 1781.
2. J. AVESTON, G. A. COOPER and A. KELLY, "The properties of fibre composites," Conference Proceedings, National Physical Laboratory, Guildford (IPC Science and Technology Press, 1971) pp. 15–26.
3. D. B. MARSHALL, B. N. COX and A. G. EVANS, *Acta Metall.* **33** (1985) 2013.
4. L. N. MCCARTNEY, *Proc. R. Soc. Lond.* **A409** (1987) 329.
5. Y. C. GAO, Y. W. MAI and B. COTTERELL, *J. Appl. Math. Phys. (ZAMP)* **39** (1988) 550.
6. S. DANCHAIVIJIT and D. K. SHETTY, *J. Am. Ceram. Soc.* **76** (1993) 2497.
7. Y. C. CHIANG, A. S. D. WAND and T. W. CHOU, *J. Mech. Phys. Solids* **41** (1993) 1137.
8. N. SHAFRY, D. G. BRANDON and M. TERASAKI, *Euro-Ceramics* **3** (1989) 3.453.
9. P. G. CHARALAMBIDES and A. G. EVANS, *J. Am. Ceram. Soc.* **72** (1989) 746.
10. C. H. HSUEH, *Mater. Sci. Eng.* **A159** (1992) 65.
11. R. MUKI and E. STERNBERG, *Int. J. Solid. Struct.* **6** (1970) 69.
12. C. H. HSUEH, *J. Mater. Sci. Lett.* **7** (1988) 497.
13. L. N. MCCARTNEY, *Proc. R. Soc. Lond.* **A425** (1989) 215.
14. B. BUDIANSKY, J. W. HUTCHINSON and A. G. EVANS, *J. Mech. Phys. Solids* **34** (1986) 167.
15. J. D. ESHELBY, *Proc. R. Soc.* **A241** (1957) 376.
16. D. B. MARSHALL and A. G. EVANS, *J. Am. Ceram. Soc.* **68** (1985) 225.
17. R. Y. KIM and N. J. PAGANO, *ibid.* **74** (1991) 1082.
18. R. A. LOWDEN and D. P. STINTON, *Ceram. Eng. Sci. Proc.* **9** (1988) 705.
19. R. N. SINGH, *J. Am. Ceram. Soc.* **73** (1990) 2930.
20. T. W. CLYNE and A. J. PHILLIPPS, *Compos. Sci. Technol.* **51** (1994) 271.
21. J. J. BRENNAN and K. M. PREWO, *J. Mater. Sci.* **17** (1982) 2371.

Received 22 December 1994
and accepted 2 May 1995